On the EM Algorithm and Bootstrap Approach Combination for Improving Satellite Image Fusion

Tijani Delleji, Mourad Zribi, and Ahmed Ben Hamida

Abstract—This paper discusses EM algorithm and Bootstrap approach combination applied for the improvement of the satellite image fusion process. This novel satellite image fusion method based on estimation theory EM algorithm and reinforced by Bootstrap approach was successfully implemented and tested. The sensor images are firstly split by a Bayesian segmentation method to determine a joint region map for the fused image. Then, we use the EM algorithm in conjunction with the Bootstrap approach to develop the bootstrap EM fusion algorithm, hence producing the fused targeted image. We proposed in this research to estimate the statistical parameters from some iterative equations of the EM algorithm relying on a reference of representative Bootstrap samples of images. Sizes of those samples are determined from a new criterion called 'hybrid criterion'. Consequently, the obtained results of our work show that using the Bootstrap EM (BEM) in image fusion improve performances of estimated parameters which involve amelioration of the fused image quality; and reduce the computing time during the fusion process.

Keywords—Satellite image fusion, Bayesian segmentation, Bootstrap approach, EM algorithm.

I. INTRODUCTION

IMAGE fusion is the technique by which a set of input images coming from different sensors or modalities or some of their features, are combined together to form a single composite fused image [1, 2, 12]. It has become an important procedure in satellite image analysis and the remote-sensing [4]. In the remote sensing domain, every band of data collected by a sensor contains some important and unique information. We know that a target interferes differently according to the length of wave of the incidental energy that where reflected, absorbed, and distributed or broadcasted in different proportions. The appearance of a target can change easily with time, sometimes in some seconds. For several applications, using information from different sources of data, guarantees

the correct identification of the target and a data picking as precise as possible. Specialists of the analysis of satellite image use multi-spectral, multi-sensor and multi-temporal manners, to fuse several sets of data, in order to extract the best possible information of a target or a region. Scientists use fused images in several applications, to determine the state of vegetation, to supervise variations of temperature in masses of water, to localize damage in an underground pipeline, and to study the soil and the basement geography. Due to the big diversity methods [7, 8, 9, 10], the fusion results fluctuate with the selected technique. But in recent years, many researchers have begun to focus on studying probabilistic based image fused algorithm. Sharma [5, 6] proposed a Bayesian fusion method, which is based on estimation theory and assumes all distortions follow a Gaussian density. Yang [3] presented an algorithm based on the assumption that all distortions best fit Gaussian and non-Gaussian. Liu [2] developed the EM algorithm only to estimate fused image in the lowest frequency band.

The major problem of these methods is the delay of computing time, especially in satellite image (because of big memory size). To resolve this problem, we apply a model called Bootstrap to the estimation algorithms. It's a resampling method that improves estimator properties notably in small samples. Zribi [16] says that to estimate the parameters' models, we replace the observed image by a Bootstrap sample of pixels drawn randomly.

In this paper, we develop a hybrid criterion to determine the optimum size of the representative Bootstrap sample [27]. The organization of this paper is as follows. In section II, we describe the Bootstrap sampling method. In section III , we discus the interest of Bootstrap approach in image analysis. In section IV, we present the Bootstrap EM algorithm for image segmentation and fusion. The metrics of quality comparison (blind metrics) between the classical EM and the Bootstrap EM (BEM) are given in section V. The results of segmentation and fusion of satellite images are shown in section VI. Finally, we present our conclusion in section VII.

II. BOOTSTRAP SAMPLING METHOD

The Bootstrap was introduced by Efron [18] as a tool for estimating the sample distribution of statistics when standard methods cannot be applied. An important aspect of this technique is that it sets researchers free from making unverifiable and most likely invalid assumptions about their

data (e.g. probability distribution) prior to analysis. The basic idea underlying the Bootstrap is to produce a random sample (called *Bootstrap sample*), which is obtained by sampling, with replacement, from the original pool of data. The Bootstrap sample is then used to compute the estimate of the parameter the researcher is interested in, and this procedure (extraction of the random sample and computation of the estimate) is repeated many times in order to create an empirical distribution of the statistic. Such a distribution usually represents a good approximation of the true (and unknown) probability distribution underlying that statistic [21].

For example to estimate a parameter Θ (like the mean, the variance or the quintile…) from a sample of size n, $X = (X_1, X_2,....., X_n)$ with unknown probability distribution F, we generate from X a Bootstrap random sample $X^* = (X_1^*, X_2^*,.....,X_n^*)$. The simulation is made according to the empirical distribution function F_n of X, that gives the probability $1/n$ for every element. The precision of the estimator is determined by a simulation of B Bootstrap samples from a sample X [20].

III. IMPORTANCE OF BOOTSTRAP IN IMAGE ANALYSIS

Many researches have applied the Bootstrap method in pattern classification [21, 22]. In this section, we present the principle of this method in image and the new representative criterion.

A. Principle

In the domain of the Bootstrap, we consider the image as a finite population with N observations is that noted by $X = (x_1, x_2,....., x_N)$ with $N = N_r \times N_c$. The N_r and the N_c represent respectively the line number and the columns number of image. Each observation takes its values in a finite set of Gray levels G. We suppose that the image is our initial sample of unknown law distribution. We draw randomly and with replacement a representative Bootstrap sample $X^* = (x_1^*, x_2^*,....., x_n^*)$ from the initial sample. This model of sampling gives the possibility to simulate a realization that presents a big interest for the evaluation of parameters. Every image is characterized by a set $G = (g_1, g_2,....., g_K)$ of levels of different Gray value. A Gray level g_i is characterized by a prior apparition probability p_i in the image. This probability can be estimated by its proportion in a Bootstrap sample of optimum size determined in our work by a new representative criterion.

B. A New Representative Criterion

1) Stratification: By the use of a composite of two probabilistic sampling techniques (random simple and stratified), we develop a hybrid criterion for the determination of the optimum size n of the representative Bootstrap sample.
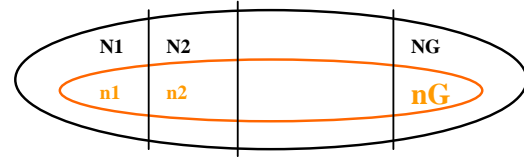

Fig. 1 The process of sampling

In Fig. 1, N_1, N_2,…….., N_G represent the stratum size and n_1, n_2,……, n_G represent the sample size where G is the number of classes. These stratum sizes and these sample sizes verify respectively the following equations:

$$N = \sum_{g=1}^{G} N_g \qquad (1)$$

and

$$n = \sum_{g=1}^{G} n_g \qquad (2)$$

The hybrid criterion [27] is a process of sampling where the population is distributed in homogeneous sub-groups or in strata (G) and where the drawing of samples is independent in every stratum.

2) Determination of the Optimal Sample Size: We use the simple random sampling to draw sub-samples (there is G sub-samples) from the total population strata. The sub-sample will be called "representative" if it assures the proportional distribution of individuals, that is to say:

$$\frac{n_g}{n} = \frac{N_g}{N} \Rightarrow \tau_g = \frac{n_g}{N_g} = \frac{n}{N} \Rightarrow n = N\tau_g \qquad (3)$$

Improving more the expression of *n*:

$$G \times n = N \times \sum_{g=1}^{G} \frac{n_g}{N_g} \Rightarrow n = \frac{N}{G} \times \sum_{g=1}^{G} \frac{n_g}{N_g} \qquad (4)$$

After that, we can apply one of the criterions given in [5] to determine the optimal size of a sub-sample drawn from a stratum. In this work, we choose the following criterion: a sample $(x_1^*, x_2^*,....., x_n^*)$ of n size will be representative of the entire image only if each Gray level appears at least one time during n drawing, thus the following expression is deduced:

$$n_g > 4 \times K_g \qquad (5)$$

K_g represents the Gray level number in a g stratum.

The expression of n will be in the following form:

$$n > \frac{4N}{G} \times \sum_{g=1}^{G} \frac{K_g}{N_g} \qquad (6)$$

IV. THE BOOTSTRAP EM ALGORITHM

A. The BEM Algorithm for Image Segmentation

In this section, we present the basic idea of the univariate gaussian mixture model and the BEM segmentation algorithm.

1. Univariate Gaussian Mixture Model

In univariate Gaussian mixture model [23], one-dimensional observations x_i are assumed to be drawn from K classes. Each of them is a Gaussian distributed. The probability density for this model is:

$$f(x_i) = \sum_{k=1}^{K} p_k f_k(x_i / \theta_k) \qquad (7)$$

where $\theta_k = (\mu_k, \sigma_k^2)^t$, $f_k(./\theta_k)$ is a Gaussian density with mean μ_k and variance σ_k^2 and $(p_1,........,p_K)$ is a vector of mixture probabilities such that $p_k \geq 0$, $k=1,......,K$ and $\sum_{k=1}^{K} p_k = 1$.

The expression of the Gaussian density $f_k(./\theta_k)$ is:

$$f_k(x/\theta_k) = \frac{1}{\sigma_k \sqrt{2\pi}} e^{-\frac{(x-\mu_k)^2}{2\sigma_k^2}} \qquad (8)$$

The estimation of a priori probabilities p_k and function parameters θ_k can be realized by using the EM algorithm [24, 25]. It is an iterative procedure designed to find the maximum likelihood estimates [22] in the context on parametric models.

2. The BEM Segmentation Algorithm

The Bootstrap EM (BEM) algorithm is proposed to estimate the parameters of mixture from a representative Bootstrap sample of a given image [27]. The mixture density of a random variable $X^* = (x_1^*, x_2^*, ..., x_n^*)$ is defined by the following form:

$$f(x^*) = \sum_{k=1}^{K} p_k f_k(x^*/\theta_k) \qquad (9)$$

The application of the BEM algorithm to image segmentation consists in the following steps:

(a) Determination of the optimal size of Bootstrap sample.
(b) Drawing with replacement of a representative Bootstrap sample of size $n<N$ from the totality of the image.
(c) Resampling of B samples from the initial sample.
(d) Application of the EM algorithm to estimate parameters of the simulated Bootstrap samples.

(i) *Initialization*: the first step is the initialization of a priori probabilities, averages and variances of every class. With the help of the image histogram or the K-Means Clustering method, we initialize those parameters in the following way:

$$\hat{p}_k^0 = \frac{\hat{n}_k^0}{n}; \hat{\theta}_k^0 = (\mu_k^0, \sigma_k^0) \qquad (10)$$

where $\hat{n}_k^0$ is the total number of observations in the class k.

(ii) *Expectation*: in this step we estimate the a posterior distribution $\hat{p}_k^m(x_i^*)$ for the pixel x_i^* that belongs to the class k at the mth iteration by:

$$\hat{p}_k^m(x_i^*) = \frac{1}{n} \sum_{i=1}^{n} \hat{p}_k^m \qquad (11)$$

(iii) *Maximization*: at the $(m+1)$th iteration we can estimate the a priori probability $\hat{p}_k^{m+1}$, the mean $\hat{\mu}_k^{m+1}$ and the variance to each class by:

$$\hat{p}_k^{m+1} = \frac{1}{n} \sum_{i=1}^{n} \hat{p}_k^m(x_i^*) \qquad (12)$$

$$\hat{\mu}_k^{m+1} = \frac{\sum_{i=1}^{n} x_i^* \hat{p}_k^m(x_i^*)}{\sum_{i=1}^{n} \hat{p}_k^m(x_i^*)} \qquad (13)$$

$$(\hat{\sigma}_k^{m+1})^2 = \frac{\sum_{i=1}^{n} (x_i^* - \hat{\mu}_k^{m+1})^2 \hat{p}_k^m(x_i^*)}{\sum_{i=1}^{n} \hat{p}_k^m(x_i^*)} \qquad (14)$$

The algorithm stops when the condition:

$$\left| \hat{p}_k^{m+1} - \hat{p}_k^m \right| < \varepsilon \qquad (15)$$

is satisfied, with ε is a given small number.

(e) Classification: The Bayesian Rule (BR).

After the mixture identification, the BR is applied in order to classify the pixels according to their gray level x^*:

$$k(x^*) = \arg\left[\max_{1 \le k \le K}\left\{p_k f(x^*/\theta_k)\right\}\right] \qquad (16)$$

where $k(x^*)$ represents the label of the class of the pixel x^*.

3. Region Analysis

The BEM algorithm is applied separately to each input image to obtain region maps for each one. The region maps for different sensor images are generally different, because these images can come from diverse modalities. Input images may contain different objects which may appear with different shapes on input images [11]. Thus we need to determine a joint region map for the merged image.
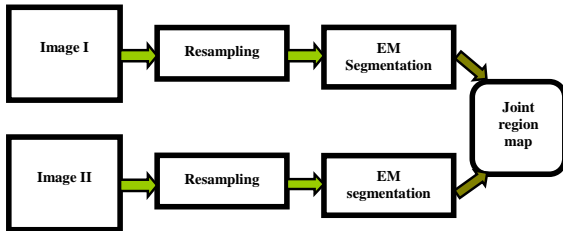

Fig. 2 Diagram of joint region map generated by the representative samples based on segmentation EM algorithm

B. The BEM Algorithm for Image Fusion

We assume that the input images are modeled as the true scene corrupted by a Gaussian mixture noise. To determine the parameters of distortion, we apply a new method called BEM fusion algorithm.

1. Image Formation Model

The image formation model is determined for each region in the joint region map. This model is defined for each pixel $j=1,\ldots\ldots,L$ in a region [2] as:

$$z_i(j)=\beta_i(j)S(j)+\alpha_i(j)+\varepsilon_i(j) \qquad (17)$$

where $i=1,\ldots..,q$ indexes the sensors; L is region size; $Z_i(j)$ is the input sensor image region; $S(j)$ is the true scene region which we hope to estimate using the fused method; $\beta_i=+1,-1$ or 0 is the sensor selectivity factor which indicate that the model acknowledges that a given sensor may be able to "see " this object ($\beta_i=+1$), may fail to "see" this object ($\beta_i=0$), or may "see" this object with a polarity reversed representation($\beta_i=-1$), $\alpha_i(j)$ is the sensor bias or the formation distortions of sensors, and $\varepsilon_i(j)$ is the random

distortion. The noise is modeled as a K–term mixture of Gaussian probability functions (pdfs) as:

$$f_{\varepsilon_i(j)}(\varepsilon_i(j)) = \sum_{k=1}^{K} \lambda_{k,i}(j)\frac{1}{\sqrt{2\pi\sigma_{k,i}^2(j)}}e^{-\frac{\varepsilon_i(j)^2}{2\sigma_{k,i}^2(j)}} \qquad (18)$$

2. BEM Fusion Procedure

The BEM algorithm proposes to estimate the model parameters from representative Bootstrap samples of each region of images. Therefore, instead of considering the region like an observation sample as the fact of the classic EM algorithm; the BEM replaces the observed region $Y = (y_1, y_2,\ldots\ldots, y_M)$ that has a size equal to M by a m-size representative Bootstrap sample $Y^* = (y_1^*, y_2^*,\ldots\ldots, y_m^*)$ selected randomly.

The application of the BEM algorithm to images regions consists in the following steps:
We follow the following steps to apply the BEM algorithm about images regions

a) Determination of the optimal size of Bootstrap sample of a region.
b) Drawing with replacement of a representative bootstrap sample of size $m<M$ from the totality of a region.
c) Resampling of B samples from the initial sample
d) Application of the EM algorithm [2, 3, 11] to estimate parameters of the simulated bootstrap samples.

◆*Initialization of parameters*: the initial values of the parameters are needed to start the EM algorithm. We estimate for the region of a true scene $S(l)$ that comes from the weighted average of the input images. A simple initialization of β_i is to assume that the region appears in each sensor image [2, 3, 11]. In order to initialize the distortion parameters the distortion is supposed impulsive. The initialization for the sensor bias α_i is to come from the average of gray level of each source image-region.

◆*Calculate of conditional probabilities*: $g_{k,i,l}[z_i(l)]$.

◆*Update selectivity factors*: β_i to β_i'.

◆*Update distortions parameters*: $\lambda_{k,i}$ to $\lambda_{k,i}'$; $\sigma_{k,i}^2$ to $\sigma_{k,i}'^2$ and α_i to α_i'.

◆*Update true region of a scene*: $S(l)$ to $S'(l)$.

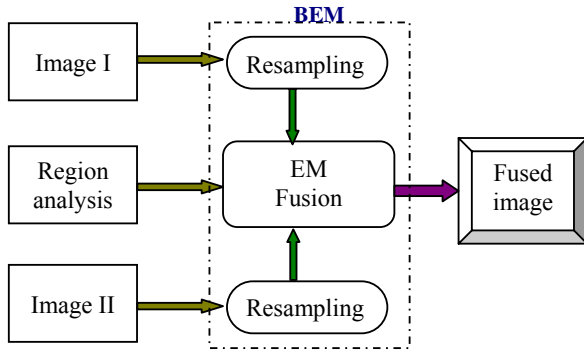e) Joint of the updated regions of a true scene

Fig. 3 Diagram of Bootstrap EM (BEM) fusion

V. PERFORMANCE COMPARISON

A. The Probability of Error Classification

We compare the performance between the classical EM algorithm and the proposed Bootstrap EM (BEM) on a Gaussian mixture which is composed of three classes. We use a significant and easy criterion proposed by Zribi in [17] to estimate the probability of error of classification which called the rate of misclassifying τ defined by:

$$\tau = \frac{number\ of\ misclassified\ pixels}{total\ number\ of\ pixels}.$$

B. Metrics to Measure the Fusion Quality

The widespread use of image analysis (segmentation, fusion, etc) methods, in military applications, in medical diagnostics, in remote sensing, etc, has led to a rising demand of applicable quality evaluation metrics in order to compare the results gotten with different algorithms [15]. Quality evaluation of images processing is often carried out by human visual inspection [13].

In this work, we apply the objective fusion performance measures (blind metrics) introduced by Pielle [15]. Piella used the image quality index Q_0 that was introduced by Wang and Bovik in [14] to define some new objective measures for image fusion which do not require a reference image: the fusion quality index and the weighted fusion quality index.

We note by $Q(a,b,f)$ the quality index, where a and b are the two input images and f is the fused image and by $s(a\backslash w)$ the some saliency of image a in a window w. The $s(a\backslash w)$ should reflect the local relevance of image a within the window w, and it may depend on (e.g. contrast, sharpness, or entropy). We note by $\lambda(\omega)$ the local weight that indicates the relative importance of image a compared to image b. A typical choice for $\lambda(\omega)$ is:

$$\lambda(w) = \frac{s(a\backslash w)}{s(a\backslash w) + s(b\backslash w)} \qquad (19)$$

then, $Q(a,b,f)$ is defined as:

$$Q(a,b,f) = \frac{1}{W}\sum_{w\in W}(\lambda(w)Q_0(a,f\backslash w) + (1-\lambda(w))(b,f\backslash w)) \qquad (20)$$

where W is the family of all windows.
From eq. (20), we define the weighted fusion quality index $Q_W(a,b,f)$ by:

$$Q_w(a,b,f) =$$
$$\sum_{w\in W} c(w)[\lambda(w)Q_0(a,f\backslash w) + (1-\lambda(w))Q_0(b,f\backslash w)] \qquad (21)$$

where,

$$c(w) = \frac{C(w)}{\sum_{w'\in W} C(w')} \qquad (22)$$

and,

$$C(\omega) = \max(s(a\backslash\omega) + s(b\backslash\omega)) \qquad (23)$$

We choose the variance and the entropy to calculate the relevance $s(a\backslash w)$ of an image. The variance denoted by σ_x^2 is an arbitrary measurement being used for characterized the dispersion (the measure of the homogeneity) of the pixels values of an image (or a window (w) in our case) defined by:

$$\sigma_x^2 = \frac{1}{n-1}\sum_{i=1}^{n}(x_i - \overline{X})^2 \qquad (24)$$

with

$$\overline{X} = \frac{1}{n}\sum_{i=1}^{n} x_i \qquad (25)$$

where n is the image size; x_i the pixel value; and $\overline{X}$ the mean of pixels values in a window.
The Entropy denoted by (H) of an image is the measurement of information present in an image (or in a window) and is defined as follows [26]:

$$H = -\sum_{i=0}^{L} p(i)\log_2 p(i) \qquad (26)$$

where L is the gray level of the image, $p(i)$ is the ratio of the number of pixels n_i with gray level i and the total number n of pixels in the image; $p(i) = n_i/n$.

VI. EXPERIMENTAL RESULTS

In this section we present some examples of unsupervised segmentation and fusion of simulated image and real images. The simulated image given in Fig. 4a is a 256*256 pixel resolution and it is constituted by three classes. These classes are corrupted by a Gaussian white noise of mean **m** and variance **v**. The default is zero mean noise with 0.01 variance. So we obtain the image assigned in Fig. 4b. We identify the mixture of three Gaussian laws of the simulated image by the

classical EM algorithm and the proposed Bootstrap EM algorithm (see; Fig. 5a and Fig. 5b).

To calculate the parameters of segmentation or fusion of the real images, we used the representative samples with sizes determined in Table I.

TABLE I
OPTIMAL SIZE OF BOOTSTRAP SAMPLE

Real Images	N image size	G stratum number	K Gray levels number	n sample size
band_L	250000	4	256	1075
band_C	250000	4	255	1471
Band1	30000	4	250	1906
Band4	30000	4	256	1124

TABLE II
DIFFERENT SIZES OF BOOTSTRAP SAMPLE FOR THE SAME IMAGE

	G strata number	n sample size
	3	1076
	4	1124
Image "Band4	5	1288
	6	1386
	7	1445
	8	1504

By an over look on tables (Table I and Table II), we notice that the hybrid criterion holds in consideration: the size N of the image, the distribution of Gray levels in every stratum, and the G number of strata, to determine the optimal size of sample Bootstrap. The optimal number of strata varies according to the image homogeneity.

Table III shows the percentage of misclassified pixels of every class obtained by the classical EM and the new approach applied to image Fig. 4a. Table IV represents the initial parameters of image Fig. 4a, the estimates of the parameters using the two algorithms (EM and BEM) and the rate of misclassifying of segmentation error rates.

To assess the performance of the new approach (BEM) we consider two pair of real images; these images are represented by 256GLs.

The first pair of test images is constituted of:

● "L-band" image (23 cm) (see Fig. 6a) is a satellite image of 500*500 pixel resolution from JERS-1 (Japan Earth Resources - 1 Satellite).

● "C-band" image (5-6 cm) (see Fig. 6b); this is an image data of 500*500 pixel resolution from Radar sat – 7.

The second pair of test images incorporates:

● "Band1" image (see Fig. 7a) is an image of 200*150 pixel resolution. The spectral response of Band 1 is in the visible portion of the electromagnetic spectrum that corresponds with blue-green light. This band is capable of being transmitted through water and is especially sensitive to particles suspended in water.

● "Band4" image (see Fig. 7b) is an image of 200*150 pixel resolution. The spectral response of Band 4 is in the Near Infrared (NIR) portion of the electromagnetic spectrum. This form of radiation is reflected to a high degree of leafy vegetation since chlorophyll reflects much of the NIR that reaches it.

Fig. 6d and Fig. 6e (resp. Fig. 7d and Fig. 7e) show the segmented images of Fig. 6a and Fig. 6b (resp. Fig. 7a and Fig. 7b) respectively. Fig. 6f (resp. Fig. 7f) shows the joint region map of the fused images Fig. 6d and Fig. 6e (resp. Fig. 7d and Fig. 7e). Fig. 6c (resp. Fig. 7c) is the fused image using the classical EM fusion algorithm.

In order to decrease the great dependence of neighbor pixels of the real images, it is more suitable to select randomly representative samples from the regions of input images instead of considering the total number of pixels. After that, we generate some resamples B (artificial samples) from these representatives' samples. Fig. 6g, Fig. 6h and Fig. 6k (resp. Fig. 7g, Fig. 7h and Fig. 7k) are the fused images obtained by using the BEM fusion algorithm; with a variation of the number of artificial samples B. This kind of sample selection is considerably reduces the fusion time (see: Table V and Table VI).

The sample selection process in BEM leads to a great improvement in maximum likelihood parameter estimation. From which comes the improvement of the fused image quality (see: Table VII and Table VIII).

VII. CONCLUSION

We have presented a new Bayesian fusion method based on EM algorithm and a Bootstrap approach combination. The Bootstrap sampling model that has been used allows an estimation of parameters of image from a representative sample. The size of optimal sample is determined by the proposed new criterion called: hybrid criterion. The results of different satellite images presented in this work show the advantage of Bootstrap approach in satellite image fusion or even in segmentation. The interest in Bootstrap-EM (BEM) assessment of satellite images is an original approach which was successfully implemented and tested.

Obtained results of our work show that using BEM approach in image fusion improves performances of estimated parameters which involve amelioration of the fused image quality; and reduce the computing time during the fusion process.

REFERENCES

[1] Z. Zhang and R. S. Blum, "A categorization of multiscale decomposition based image fusion scheme with a performance study for a digital camera application" Proceedings of the IEEE, Vol. 87, no.8, pp.1315- 1326, August 1999.
[2] G. Lui, Z. L. Jing, J. X. Li, S. Y. Sun Z. H . Li and H. Leung, "image fusion based on estimation theory", Proceedings of the third international conference on machine learning and cybernetics, Shanghai, pp. 26-29, August 2004.
[3] J. Yang and R. S. Blum, " a statistical signal processing approach to image fusion for concealed weapon detection", Proceedings of the IEEE international conference on image processing, Rochester, NY, pp. 513-516, 2002.
[4] G. Simone, A. Farina, L. Morabito, S. Serpico, and L. Bruzzon, "image fusion techniques for remote sensing applications", information fusion, Vol. 3, no.1, pp. 3-15, 2002.
[5] R. K. Sharma, "probabilistic model-based multisensor image fusion", PHD dissertation, Oregon graduate institute, Portland, OR, October 1999.
[6] R. K. Sharma, T. K. Leen and M. Pavel, "probabilistic image sensor fusion", advances in neural information processing systems, Vol.11, the MIT Press, 1999.

[7] L. Bin and P. Jiaxiong, "image fusion method based on short support symmetric non-separable wavelet", international journal on wavelets, multiresolution and information processing, Vol.2, no.1, pp.87-98, 2004.

[8] Z. Zhang and R. S. Blum, "region-based image fusion scheme for concealed weapon detection", proceedings of the 31st annual conference on information sciences and systems, march 1997.

[9] J. J. Lewis, R. J. O'callaghan , S. G. Nikolov, D. R. Bull and C. N. Canagarajah", region based image fusion using complex wavelats ", in 7 th international conference on information fusion , Stockholm, Sweden, 28 June, 2004.

[10] A. Akerman, "pyramidal techniques for multisensor fusion", Proceedings of SPIE; Volume 1828 Sensor Fusion V, pp.124-131, USA November 1992.

[11] J. Yang and R. S. Blum, "A Region based Image Fusion Method using the Expectation-Maximization Algorithm", Information Sciences and Systems, 40th annual conference on, pp. 468-473, 2006.

[12] S. G.Nikolov, J. J. Lews, R. G. O'Callaghan, D. R. Bull and C. N. Canagarajah, "Hybrid Fused Displas: Between Pixel-and Region-Based Image Fusion", the 7th International conference on information fusion, Stokholm, Sweden, 2004.

[13] A. Toet and E. M. Franken, "Perceptual of different image fusion schmes", Displays, Vol. 24, no. 1, pp. 15-37, February 2003.

[14] Z. Wang and A. C. Bovik, "A universal image quality index", IEEE signal processing letters, Vol. 9, no.3, pp. 81-84, march 2002.

[15] G. Piella and H. Heijmans, "A new quality metric for image fusion", Image processing Proceedings, Vol. 3, pp. 173-6, 2003.

[16] M. Zribi, "Non parametric and unsupervised Bayesia classification with Bootstrap sampling", Image and Vision Computing, 22, pp.1-8, 2004.

[17] M. Zribi, F. Ghorbal, "An unsupervised and nonparametric Bayesian classifier", Pattern Recognition Letters, Vol. 24 pp. 97-112, 2003.

[18] B. Efron, "Bootstrap methods: another look at the Jackknife", Ann. Stat. 7 (1), 1979.

[19] B. Efron, R. J. Tibshirani, "An introduction to the bootstrap", Monographs on Statistics and Applied Probability, 57, 1993.

[20] I. Buvat, "Introduction à l'approche Bootstrap", U494 INSERM, 25 septembre, 2005.

[21] C. Banga, "L'approche Bootstrap en analyse des   images : Application à la restitution de la cinétique de la fuite en choriorétinopathie Séreuse Centrale", Thèse de doctorat, université de Rennes I, 1995.

[22] R. Veysseyre, Statistique et probabilité pour l'ingénieur, Dunod, Paris 2001.

[23] C. Ambois, "Introduction a la reconnaissance statistique des formes", Centre de Géostatique, Ecole des mines de Paris, mars1997.

[24] G. J. McLachlan, T. Krishnan, The EM Algorithm and Extensions, John Wiley and Son's Inc., New York, 1997.

[25] N. Kehtarnavaz, E. Nakamura, "Generalization of the EM algorithm for mixture density estimation", Pattern Recognition Letters 19, pp. 133-140, 1998.

[26] A. German, M. R. Jenkin, and Y. Lesperance, " Entropy-Based Image Merging", The 2nd Canadian Conference on Computer and Robot Vision (CRV'05) Toronto, Ontario, Canada, pp. 81-86, 2005.

[27] T. Delleji, Mourad Zribi and Ahmed ben Hamida, "Application of bootstrap approach Unsupervised   Statistical Segmentation of Satellite Images", 4th International Multi-Conference on Systems, Signals & Devices; SSD'2007 March 19-22, Hammamet (Tunisia), 2007.
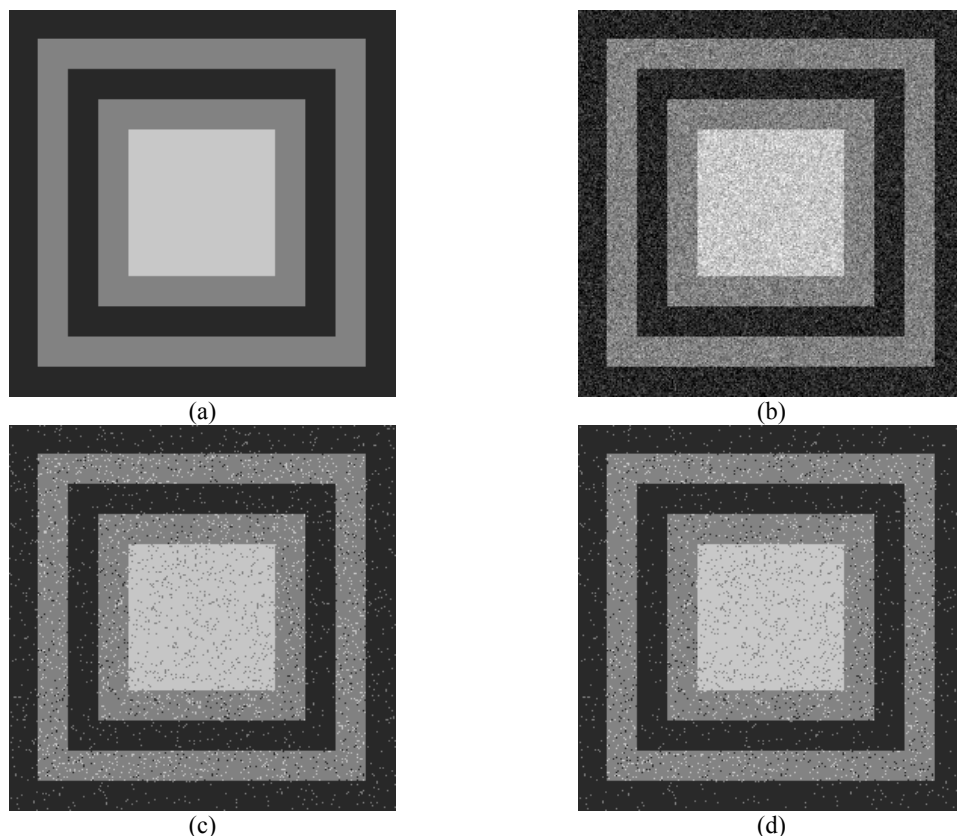
Fig. 4 (a) original image, (b) distorted image, (c) segmented image (b) with classical EM algorithm (d) segmented image (b) with BEM algorithm
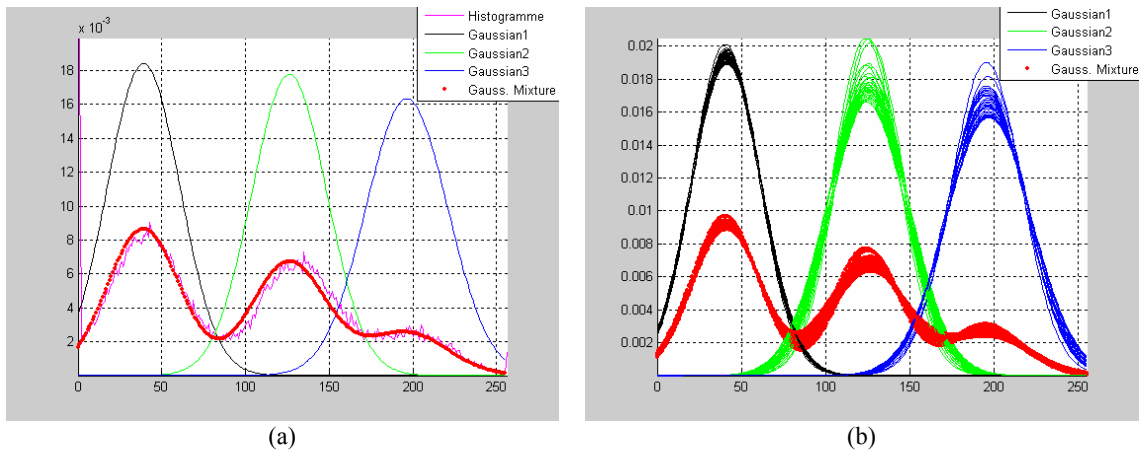
Fig. 5 (a) Gaussian mixture obtained by classical EM algorithm, (b) Gaussian mixture obtained by BEM algorithm

TABLE III
THE NUMBER OF MISCLASSIFIED PIXELS FOR CLASSICAL EM AND BEM

class	Initial pixel numbers	Classical EM		Bootstrap EM (BEM)	
		Pixels' number after segmentation	the number of misclassified pixels % every class	Pixels' number after segmentation	the number of misclassified pixels % every class
1	31007	30736	271	31043	36
2	25120	24176	944	24272	848
3	9409	10624	1215	10221	812

TABLE IV
PARAMETERS ESTIMATED FROM IMAGE FIG. 2B

Parameters	π_1	π_2	π_3	μ_1	μ_2	μ_3	σ_1	σ_2	σ_3	τ
theoretical	0.473	0.383	0.143	40	130	200	0	0	0	---
Classical EM	0.4690	0.3798	0.151	39.906	128.938	197.946	21.647	22.653	24.020	1.85
BEM	0.481	0.368	0.1498	41.235	130.5	199.956	21.104	22.544	22.642	1.29%

TABLE V
TIME OF "BAND_L" AND "BAND_C" IMAGES FUSION UNDER A STATION OF CALCUL (P4)

Fusion approach	Resample number (B)	Nunumber iteration	Compilation Time in seconds
Classical EM		3	5837.765
Bootstrap EM (EMB)	2	3	2261.188
Bootstrap EM (EMB)	10	3	2322.516
Bootstrap EM (EMB)	100	3	2395.703

TABLE VI
TIME OF "BAND1" AND "BAND4" IMAGES FUSION UNDER A STATION OF CALCUL (P4)

Fusion approach	Resample number (B)	Nunumber iteration	Compilation Time in seconds
Classical EM		3	119.93
Bootstrap EM (EMB)	2	3	21.469
Bootstrap EM (EMB)	100	3	25.828
Bootstrap EM (EMB)	1000	3	66.781

(a) band_L image   (b) band_C image   (c) Fused image by classical EM

(d) Image (a) segmented   (e) Image (b) segmented   (f) Jointe region map

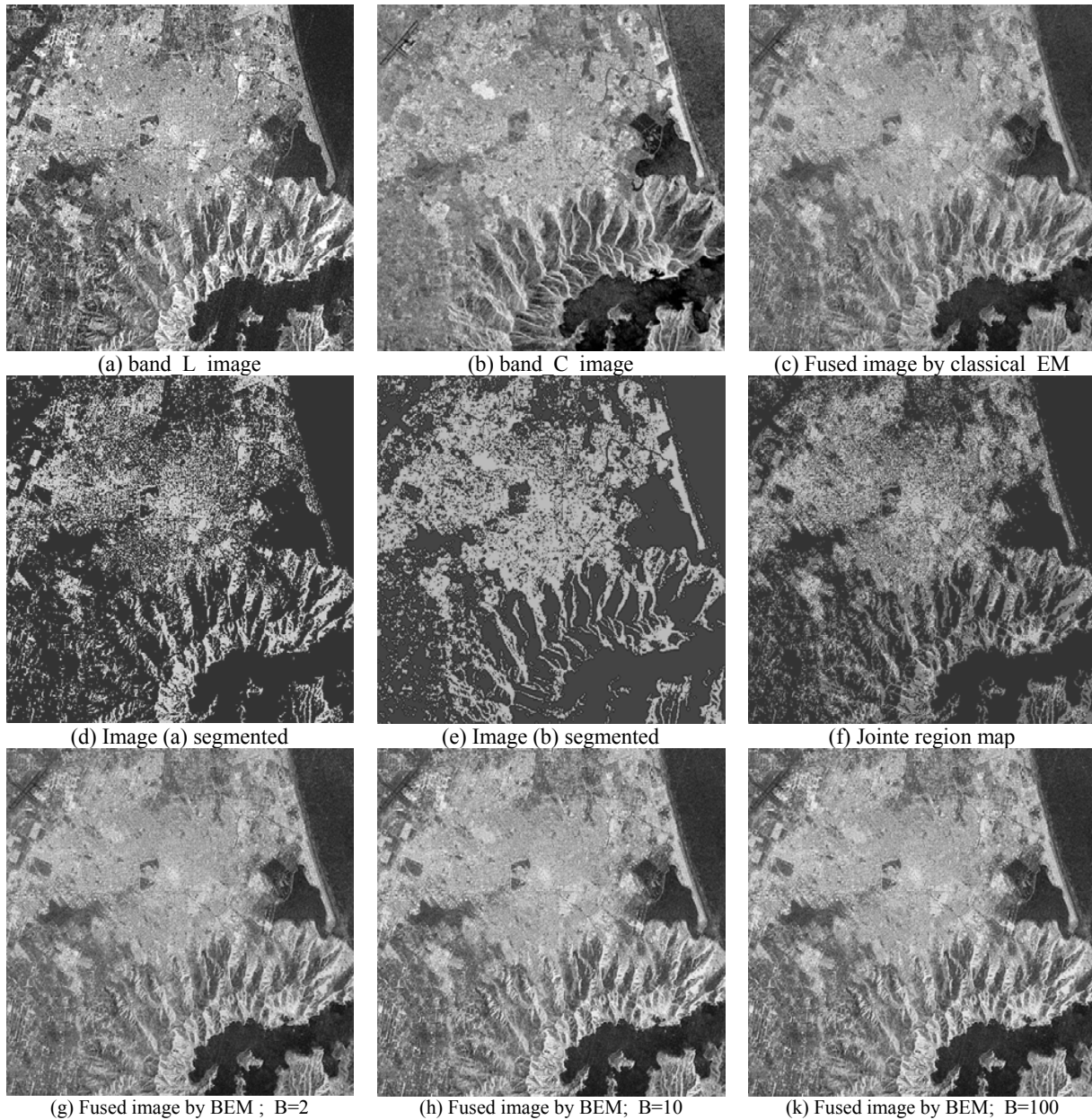(g) Fused image by BEM ; B=2   (h) Fused image by BEM; B=10   (k) Fused image by BEM; B=100

Fig. 6 fusion results on band_C and band_L images

TABLE VII
COMPARISON OF DIFFERENT QUALITY MEASURE FOR THE COMPOSITE IMAGES IN FIG. 6

metrics	The relevance s(a\w)	Classical EM	BEM; B=2	BEM; B=10	BEM;B=100
Q	The Variance	0.9110	0.9071	0.9451	0.9410
Qw	The Variance	0.9438	0.9479	0.9844	0.9796
Q	The Entropy	0.8990	0.9018	0.9265	0.9231
Qw	The Entropy	0.9051	0.9079	0.9326	0.9293

(a) Band1 image

(b) Band4 image

(c) Fused image by classical EM

(d) Image (a) segmented

(e) Image (b) segmented

(f) Jointe region map

(g) Fused image by BEM; B=2

(h) Fused image by BEM ; B=100
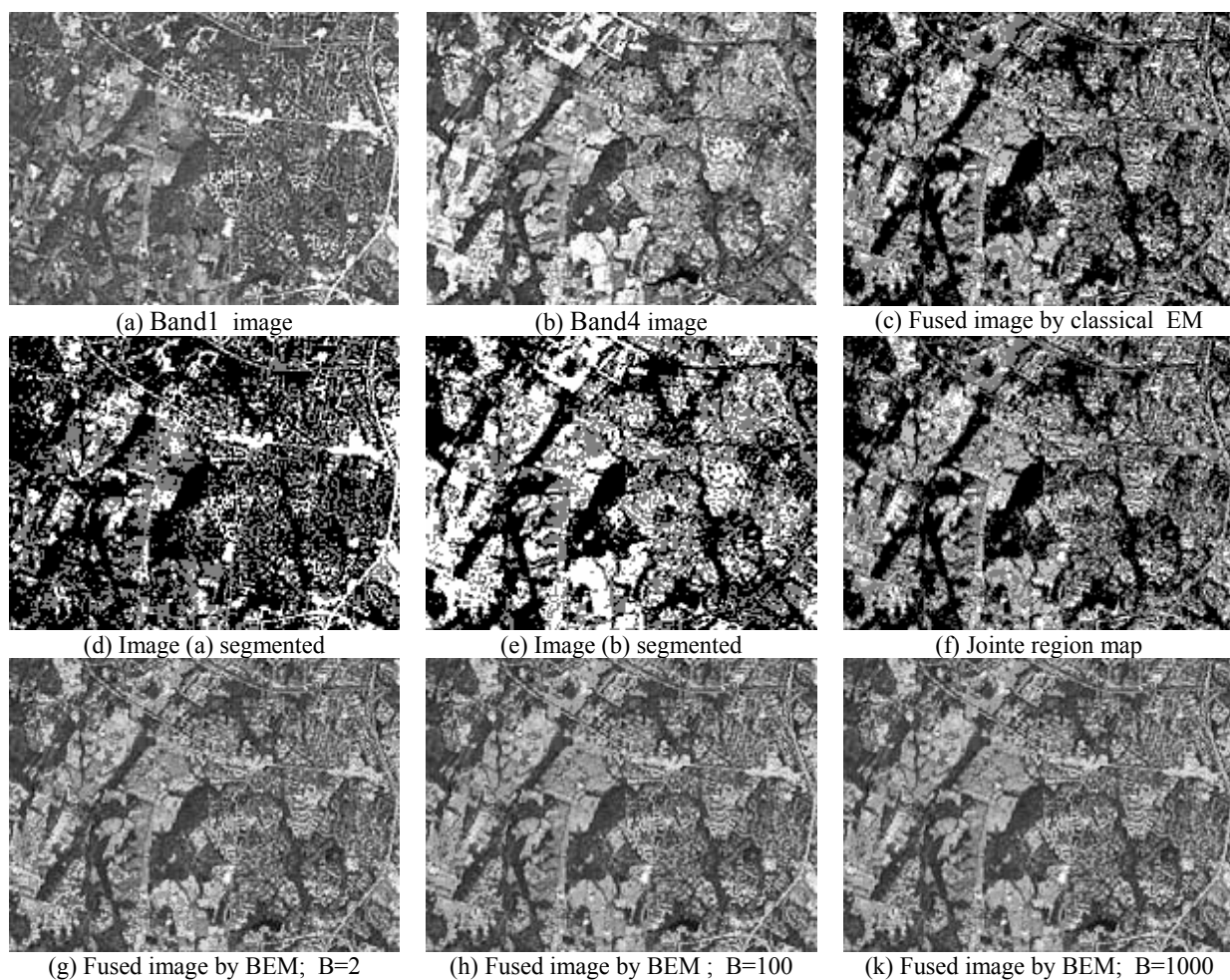
(k) Fused image by BEM; B=1000

Fig. 7 Fusion results on Band1 and Band4 images

TABLE VIII
COMPARISON OF DIFFERENT QUALITY MEASURE FOR THE COMPOSITE IMAGES IN FIG. 7

metrics	The relevance s(a\w)	Classical EM	BEM; B=2	BEM; B=100	BEM;B=1000
Q	The Variance	0.84	0.7672	0.7664	0.7656
Qw	The Variance	0.8367	0.7591	0.7568	0.7551
Q	The Entropy	0.8134	0.7565	0.7560	0.7559
Qw	The Entropy	0.8158	0.7586	0.7580	0.7580